Publication Year	2017
Acceptance in OA@INAF	2021-04-26T14:20:07Z
Title	Meeting the Challenge from Bright and Fast Gamma-Ray Flares of 3C 279
Authors	VITTORINI, VALERIO; TAVANI, MARCO; Cavaliere, A.
DOI	10.3847/2041-8213/aa767f
Handle	http://hdl.handle.net/20.500.12386/30918
Journal	THE ASTROPHYSICAL JOURNAL LETTERS
Number	843

The Astrophysical Journal Letters, 843:L23 (5pp), 2017 July 10 https://doi.org/10.3847/2041-8213/aa767f
© 2017. The American Astronomical Society. All rights reserved.

Meeting the Challenge from Bright and Fast Gamma-Ray Flares of 3C 279

V. Vittorini[1], M. Tavani[1,2,3,4], and A. Cavaliere[1,4]
[1] INAF/IAPS-Roma, via Fosso del Cavaliere 100, I-00133 Roma, Italy
[2] Universitá "Tor Vergata," Dipartimento di Fisica, via della Ricerca Scientifica 1, I-00133 Roma, Italy
[3] Gran Sasso Science Institute, viale Francesco Crispi 7, I-67100 L'Aquila, Italy
[4] Astronomia, Accademia Nazionale dei Lincei, via della Lungara 10, I-00165 Roma, Italy
Received 2017 March 22; revised 2017 May 30; accepted 2017 May 31; published 2017 July 7

Abstract

Bright and fast gamma-ray flares with hard spectra have been recently detected from the blazar 3C 279, with apparent GeV luminosities up to 10^{49} erg s^{-1}. The source is observed to flicker on timescales of minutes with no comparable optical–UV counterparts. Such observations challenge current models of high-energy emissions from 3C 279 and similar blazar sources that are dominated by relativistic jets along our line of sight with bulk Lorentz factors up to $\Gamma \sim 20$ launched by supermassive black holes. We compute and discuss a model based on a clumpy jet comprising strings of compact plasmoids as indicated by radio observations. We follow the path of the synchrotron radiations emitted in the optical–UV bands by relativistic electrons accelerated around the plasmoids to isotropic Lorentz factors $\gamma \sim 10^3$. These primary emissions are partly reflected back by a leading member in the string that acts as a moving mirror for the approaching companions. Around the plasmoids, shrinking *gap* transient overdensities of seed photons build up. These are upscattered into the GeV range by inverse Compton interactions with the relativistic electrons accelerated in situ. We show that such a combined process produces bright gamma-ray flares with minor optical to X-ray enhancements. Main features of our model include: bright gamma-ray flares with risetimes as short as a few minutes, occurring at distances of order 10^{18} cm from the central black hole; Compton dominance at GeV energies by factors up to some 10^2; minimal reabsorption from local photon–photon interactions.

Key words: galaxies: active – galaxies: individual (3C 279) – galaxies: jets – gamma rays: galaxies – gamma rays: general

1. Introduction

The flat-spectrum radio quasar (FSRQ) 3C 279 ($z = 0.536$) is a blazar prominent in gamma-rays. It was repeatedly detected above 100 MeV by EGRET (Hartmann et al. 1992; Kniffen et al. 1993), AGILE (Giuliani et al. 2009), and *Fermi*-LAT (e.g., Hayashida et al. 2012, 2015), and also detected above 100 GeV by MAGIC (Albert et al. 2008). In 2015 June, 3C 279 was caught in a remarkably bright flaring state by Ackermann et al. (2016, hereafter A16). The apparent gamma-ray luminosity attained 10^{49} erg s^{-1} (under isotropy assumption), with flux variability timescales resolved down to 2–3 minutes and doubling times of ∼5 minutes.

In fact, the overall gamma-ray activity observed in 3C 279 by Hayashida et al. (2015) and by A16 in 2015 June shows strongly enhanced radiation above 100 MeV lasting several days. Several features are to be noted: a very high "Compton dominance" in the spectral energy distribution, marked by a ratio of gamma-ray to optical emission rising by factors 3–5 to attain values $q \sim 10^2$ in a few hours; very rapid flickering with resolved timescales down to a few minutes; a flat gamma-ray spectrum occasionally extending out to about 50 GeV (Paliya 2015), with no evidence of local reabsorption. Such unprecedented features set a challenge hard to meet for most current radiative models of this source, and possibly of other blazars as well, such as PKS 1222+216 (Aleksić et al. 2011), PKS 1510-089, and 3C 454.3 (Coppi 2016).

2. Modeling the Gamma-Ray Source

Blazars are dominated by a relativistic jet with a Lorentz boost $\Gamma \sim 10$–20, launched by a supermassive black hole (SMBH) along our line of sight. They feature widely extended non-thermal spectra, which are interpreted in terms of synchrotron (S) emission and of inverse Compton (IC) radiation (cf. Rybicki & Lightman 1979); these are produced by electrons accelerated in the jet to attain random Lorentz factors up to $\gamma_b \sim 10^3$. In particular, FSRQs are often marked by gamma-ray Compton dominance, though generally at less extreme degrees than 3C 279 itself.

The S emission is observed at energies $\epsilon_s \propto \gamma_b^2\, \Gamma\, B'$ with a luminosity $L_S \sim c\, \sigma_T\, n'\, \ell'^3\, \gamma_b^2\, U'_B\, \Gamma^2$. These are given in terms of the number density $n' \sim 10^3$ cm^{-3} of energetic electrons with $\gamma_b \sim 10^3$, within the source size $\ell' \sim 10^{16}$ cm threaded by a magnetic field of strength $B' \sim 0.1$–1 G with magnetic energy density $U'_B = B'^2/8\pi \simeq 10^{-2}$ erg cm^{-3} (primed quantities refer to the comoving frame). Such emission is widely held to explain the continuum observed from the IR to *UV* bands. IC scattering is often taken into account for the gamma-ray yield from the same electron population. This operates on any density U' of soft "seed" photons present in the jet by conserving their number while upgrading their energy to yield observed luminosities $L_{IC} \sim c\, \sigma_T\, n'\, \ell'^3\, \gamma_b^2\, U'\, \Gamma^2$.

On the other hand, all FSRQs also share with the other quasars two thermal features: strong, nearly isotropic broad emission lines shining in the optical band and produced in the broad-line region (BLR), and a bright big blue bump (BBB) comprising convolved continua produced by the hot inner rings of the accretion disk surrounding the central SMBH (e.g., Peterson 1997, 2006). To wit, 3C 279 features all radiative components observed in FSRQ blazars, but during its flares the gamma-ray band is enhanced and variable to an extreme degree.

In the present Letter, we discuss the implications of these findings, and propose an interpretation of the gamma-ray flaring activity of 3C 279 in terms of a clumpy jet. The latter features strings of plasmoids as long recognized in the radio observations of this and other blazars (see Howatta et al. 2009 and references therein). Indeed, radio observations of plasmoid kinematics in 3C 279 (Howatta et al. 2009) indicate a boost $\Gamma \simeq 20$ that we adopt in the present Letter. In our model, the jet has an opening angle $\theta \sim \Gamma^{-1}$.

The short timescales $t_v \sim$ a few minutes observed in the 2015 June gamma-ray flares of 3C 279 point to emission from regions of small proper sizes $d' \lesssim c\, t_v\, \Gamma^2 \simeq 10^{13}\,\mathrm{cm}\,\Gamma^2$. High luminosity coupled with fast variability constitutes the challenge to be met by a viable source model.

A guide toward a satisfactory IC model is provided by considering the energy density of the seed photons after the pattern

$$U' = \frac{L'}{4\pi c d'^2}, \tag{1}$$

in terms of the *effective* luminosity L' of their source and of the size d' of the containing volume. It is seen that smaller size values not only enhance U', but also shorten the variability timescale, so as to achieve a substantial Compton dominance within short times. Meanwhile, smaller sizes decrease the local reabsorption of the IC radiation by photon–photon pair-producing interactions. In fact, our model focuses on physical conditions where small values of d' arise.

3. IC Radiation from BLR Seed Photons?

Meeting the above requirements while retaining the bound $\Gamma \lesssim 20$ for 3C 279 make the models limited to seed photons from the BLR problematic. Such models are based on combinations of S and IC radiated at radii $R \lesssim 0.1$ pc by a population of relativistic electrons with Lorentz factors $\gamma \lesssim 10^3$ as discussed by Hayashida et al. (2015) and A16. The electrons inhabit the jet and interact with the local magnetic field $B' \lesssim 1$ G to produce S emission, while by the IC process upscatter any seed photons of density $U'_{\rm BLR}$ as seen in the jet frame.

In the synchrotron self-Compton approach (e.g., Maraschi et al. 1992), the very same S photons are upscattered into the GeV range, to yield a basal level of IC $\sim$ S luminosities resulting in $q \sim 1$. External radiation Compton may yield larger IC emission by upscattering additional UV photons produced in the BLR at $R_{\rm BLR} \sim 0.1$ pc by BBB light reprocessed/reflected by gas clouds that float around at some 10^3 km s^{-1} within the region. The resulting energy density is given by

$$U'_{\rm BLR} \simeq (7 \times 10^{-3}\ \mathrm{erg\ cm^{-3}})\,(\xi/0.02) \times (R_{\rm BLR}/0.1\ \mathrm{pc})^{-2}\, L_{D,46}\, \Gamma^2, \tag{2}$$

where we assumed a disk luminosity $L_D = 10^{46}$ erg s^{-1} appropriate for 3C 279, a BLR covering factor $a = 0.2$ and a cloud reflectivity $f_c \simeq 0.1$ to produce $\xi = a\, f_c \simeq 0.02$. Such a value for $U'_{\rm BLR}$ may yield a ratio IC to S luminosities $q = U'_{\rm BLR}/U'_B \simeq 50$, still insufficient for explaining the 2013 December and 2015 June bright and fast gamma-ray flares of 3C 279.

On route toward higher IC/S ratios, one may consider the more abundant IR photons that are radiated by the dusty torus around the accretion disk upon reprocessing the BBB light; however, such photons are less effective than the UV ones for upscattering into the GeV range (see Böttcher et al. 2013). Alternative scenarios just make do with lower values of B and modest accelerations, but they have to assume $\Gamma > 35$ to avoid reabsorption of the meager IC radiation by photon–photon interactions within the BLR (Hayashida et al. 2015, A16).

Straightforward consequences of these models include a very *low* magnetic field $B < 0.1$ G in the jet and the related bulk magnetization $\sigma_j \propto B^2/\Gamma^2 \sim 10^{-4}$ (A16). This would imply (see, e.g., Mignone et al. 2013; Yuan et al. 2016; Cavaliere et al. 2017) it has a jet that resists forming MHD structures that are conducive to driving magnetic reconnections and micro-instabilities active for electron accelerations. In addition, these —if they somehow were driven—would be ineffective to attain high values of $\gamma \simeq 10^3$ (see Section 4). Alternative scenarios for FSRQ emissions consider special structures, such as spine-sheaths (Tavecchio & Ghisellini 2008; Sikora et al. 2016) and "rings of fire" (MacDonald et al. 2015).

We conclude that achieving substantial Compton dominance $q \sim 100$ coupled with very fast variability requires the source to have substantially higher values of U' compared with Equation (1), within far smaller volumes than can be provided by the BLR, as anticipated in Section 2 and initially discussed in Vittorini et al. 2014. Moreover, the hard unabsorbed gamma-ray spectra up to $\sim$100 GeV often observed in such sources (see, e.g., Costamante 2017) point toward emission sites beyond the BLR.

4. Enhanced Seed Photons from Moving Mirrors

Thus, we are led to develop the scenario proposed in Tavani et al. (2015). In the present Letter, we base our model on a clumpy jet with a bulk magnetization $\sigma_j \gtrsim 1$; the jet comprises a sequence of plasmoids moving out with speeds β and boosts $\Gamma \leqslant 20$. These plasmoids are related to tearing instability and reconnections of $\boldsymbol{B}$-lines in the jet that are squeezed or even invert their polarity within a collisionless plasma layer. Such processes have been widely proposed, discussed, and numerically computed (cf. Kagan et al. 2015; Coppi 2016; Lyutikov et al. 2016; Petropoulou et al. 2016; Yuan et al. 2016; see also Burch et al. 2016 for observational evidence in an astrophysical context). They form strings of separate "magnetic islands" that proceed to merge into larger and larger plasmoids. We refer to plasmoid sizes $\ell' \sim 10^{16}$ cm at a distance $R < 0.1$ pc from the central SMBH. Their origin is related to the changing topology of the $\boldsymbol{B}$-lines that induces $\boldsymbol{E}$ fields localized between plasmoids in gaps of around 10^{16} cm and shrinking. These $\boldsymbol{E}$ fields are known from a number of detailed kinetic simulations to accelerate electrons up to $\gamma \sim 10^3$ in conditions where the local electron magnetization is large, i.e., $\sigma_e > \sigma_j\, m_p/m_e \sim 10^2$.

The relative plasmoid distances in a string vary depending on their different speeds along the jet, with the leading one significantly slowed down primarily by snow-plow effects against jet material, in particular, BLR clouds. This constitutes an interesting condition as the leading member in a string can reprocess and partially reflect some of the primary S radiation emitted by the trailing members (photons "mirrored" by slow

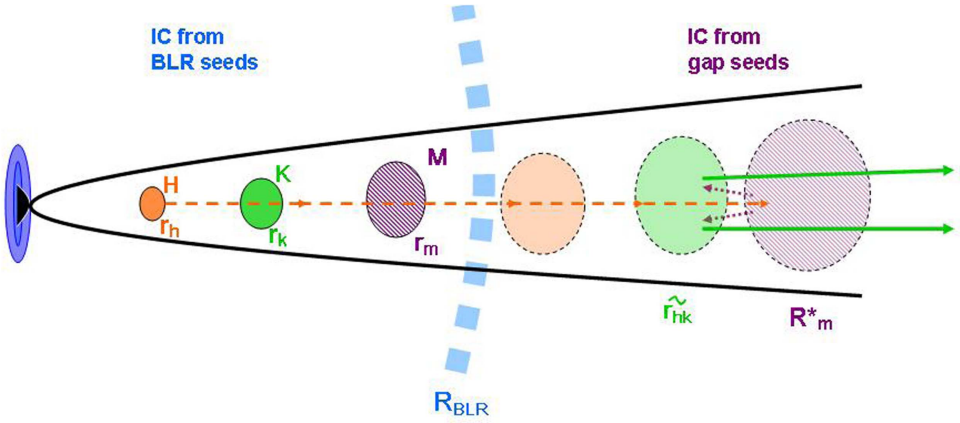

Figure 1. Schematic picture of the source structures we expect at and beyond the BLR. S radiation (orange dashed line) is emitted by inner plasmoids such as H at a radius r_h and is reflected back (violet dotted lines) by the outermost mirror-plasmoid M at a radius R_m^* toward an incoming plasmoid K: the encounter occurs at a radius $\tilde{r}_{hk}$. Dense seed photons build up in the gap between the approaching plasmoid K and the mirror, where they are IC upscattered to gamma-ray energies (green dotted lines) by electrons accelerated in and around plasmoids.

clouds in the BLR were originally proposed by Ghisellini & Madau 1996).

Shrinking mirror-plasmoid gaps so produced provide compact sites with high seed photon densities for intense IC to take place. In a scenario with multiple emitting plasmoids (see Figure 1), the primary S flux in the optical–UV bands is emitted by a plasmoid like H starting within the BLR, that is, in the range $0 < r_h < R_{\rm BLR}$. The S flux is emitted forward and mirrored backward by the leading plasmoid M toward an incoming plasmoid K. The whole process is subject to a "causality condition" (Böttcher & Dermer 1998); the mirrored photons are received by an incoming plasmoid when the latter is at the receiving point that we denote with $\tilde{r}_{hk}$ (cf. Figure 1).

The condition is easily evaluated when the same plasmoid moving with radial coordinate $r = r_0 + \beta ct$ and boost Γ first emits at r, and then receives the radiation reflected backward by the mirror moving with coordinate $r_m = r_{mo} + \beta_m ct$ and boost Γ_m. The receiving point reads $\tilde{r} = \tilde{r}_0 + r\,[(1+\beta_r)\Gamma_r]^{-2}$ in the AGN frame, for primary photons emitted in the named range and reflected back at $R_m^* = R_{m0}^* + \beta_m(1-\beta)r/[\beta(1-\beta_m)]$. Here $\beta_r = (\beta - \beta_m)(1-\beta\beta_m)^{-1}$ and correspondingly $\Gamma_r = \Gamma\Gamma_m(1-\beta\beta_m)$ are the relative velocity and boost between the receiver and the mirror (note that $\Gamma_r \simeq \Gamma/[\Gamma_m(1+\beta_m)]$). Moreover, $\tilde{r}_0 = 2(\beta r_{m0} - \beta_m r_0)\,[(1+\beta)(1-\beta_m)]^{-1}$ is the receiving point for primary photons emitted at $r \simeq 0$ and reflected at $R_{m0}^* = (\beta r_{m0} - \beta_m r_0)/[(1-\beta_m)\beta]$. Note that for small values of r_0 the approximation $R_{m0}^* \simeq 2\Gamma_m^2\, r_{m0}$ holds; so the factor Γ_m^2 makes it possible to have relevant reflections *beyond* $R_{\rm BLR}$. The IC radiative event is completed when the plasmoid K crosses the effective gap defined by

$$d_g \equiv \tilde{r} - \tilde{r}_0 = \frac{R_{\rm BLR}}{(1+\beta_r)^2\,\Gamma_r^2}, \tag{3}$$

and lasts for an observer time $t_v = d_g/[c\beta(1+\beta)\Gamma^2] \simeq R_{\rm BLR}/[8\,c\,\Gamma^2\Gamma_r^2]$: this turns out to be about 2 minutes when, e.g., $R_{\rm BLR} \simeq 3\times 10^{17}$ cm, $\Gamma \simeq 20$, and $\Gamma_r \simeq 5$ hold.

In the initial stage, the primary emitter radiates from an inner position $r \ll R_m^*$ and the mirror surface $\pi\ell_m'^2$ is small relative to the cross section of the emission beam $\pi R_m^{*\,2}\Gamma^{-2}$ as to reduce the effective power received by the mirror to $4\,L_S'\,[\ell_m'/(R_m^* - r)]^2\,\Gamma_r^4$ in the head-on approximation and with $1+\beta_r \simeq 2$. A fraction $f_m \simeq n_{\rm cold}'\sigma_T\ell_m'$ thereof is reflected back and is received by the incoming plasmoid when the latter is close to the reflection point, that is, in a cone of a cross section of order $\pi\ell_m'^2$. Then, in the gap we have

$$U_m' \simeq (5\ 10^{-5}\ {\rm erg\ cm^{-3}})\frac{f_{m,-1}L_{S,43}'\,\Gamma_r^6}{(R_m^* - r)_{18}^2}. \tag{4}$$

The denominator represents the beam dilution of the primary photons, while the volume swept per unit time is $\pi c\ell_m'^2$. Such values of U_m' are still insufficient to dominate over $U_{\rm BLR}'$ as given by Equation (2); in addition, for 3C 279 flares very short risetimes are required by A16 observations.

As the emitting plasmoid travels toward and beyond $R_{\rm BLR}$, the mirror surface fills up the primary emission cone, and the effective received power saturates to the full value $L_S'\,\Gamma_r^2$. The fraction f_m is reflected toward the incoming plasmoid until the receiving radius $\tilde{r}$ becomes very close to the reflection point. Thus, high-energy densities of seeds prevail in the comoving frame, and for primary photons emitted at $r \simeq R_{\rm BLR}$ attain a maximum that reads

$$U_m' \lesssim (2\times 10^{-1}\ {\rm erg\ cm^{-3}})\,\frac{f_{m,-1}\,L_{S,43}'\,\Gamma_r^4}{\ell_{m,16}'^2}. \tag{5}$$

We may compare the above Equations (4) and (5) with the photon energy density experienced by a plasmoid crossing the BLR, that is, with $U_{\rm BLR}'$ given by Equation (2). Remarkably, if $\Gamma \simeq 20$ holds, we have $U_m' > U_{\rm BLR}'$ for $\Gamma_r \simeq 5$ (corresponding to $\Gamma_m \simeq 2$); with such values an interesting configuration is obtained in the moving mirror scenario. We stress that high seed photon densities confined to the gap may well occur beyond the BLR, a welcome feature of our model that minimizes reabsorption by local photon–photon interactions.

5. Simulations

Our simulations treat in detail plasmoids ejected in a string along the jet with different velocities. Each member H in the string has proper size ℓ_h' and moves along the jet according to $r_h = r_{h0} + c\beta_h t$, r_h being the distance from the SMBH at time t in the AGN frame. Key elements are: (1) non-uniformity of the

plasmoid boosts in the string, with a slower leading member; and (2) the leader acts as a moving mirror that partially reflects back S radiation toward an approaching companion K.

We numerically simulate the emissions resulting from a set of values Γ_h, for h running from 1 to 6, with the upper value denoting the mirror; we use the subscripts h for the primary emitter, k for the receiver, and m for the mirror. For simplicity, we carry out the formalism in the AGN reference frame where R^*_{hm} is the distance from the central BH when the photons emitted at r_h by the plasmoid H are reflected.

The primary S emission $L'_{S,h}$ from r_h occurs at the time $t_h = (r_h - r_{h0})/(\beta_h\, c)$ and is reflected back by the moving mirror at the time

$$t^*_h = \frac{\beta_h r_{m0} - r_{h0} + r_h(1 - \beta_h)}{c\beta_h(1 - \beta_m)} \tag{6}$$

when the mirror is at the reflection point $R^*_{hm} \equiv r_{m0} + c\beta_m t^*_h$. We then take into account the causality condition for the receiving plasmoid K; accordingly, mirrored photons are received back at the time

$$\tilde{t}_{hk} = \frac{R^*_{hm} - r_{k0} + ct^*_h}{c(1 + \beta_k)}, \tag{7}$$

when the receiving plasmoid K is at $\tilde{r}_{hk} = r_{k0} + c\beta_k\tilde{t}_{hk}$. Here, the mirrored photons are IC upscattered to gamma-rays. The primary emission occurs in the range $0 < r_h < R_{\rm BLR}$; for r_h spanning this range we obtain the related receiving points, subject to the obvious condition $\tilde{r}_{hk} < r^*_k$, in terms of the radius where plasmoid K touches the mirror.

At the receiving point, the electron population of plasmoid K upscatters after the IC processes the mirrored photons originally emitted by plasmoid H. The energy density of these seed photons in the IC scattering region is

$$U'_{hk} \simeq \frac{f(1 - f)^{2N-h-k} L'_{s,(h)}\, [(1 + \beta_{r,h})\Gamma_{r,h}]^4\, \Gamma^2_{r,k}}{4\pi c(R^*_{hm} - r_h)^2}, \tag{8}$$

where N is the number of emitters in our string, $\Gamma_{r,h}$ are the relative boosts of the plasmoids relative to the mirror; note that U'_{hk} can grow until r_h becomes comparable with $R_{\rm BLR}$, as anticipated in Section 4 and detailed by Equation (5).

In Figure 2, we present an example (with $N = 5$ plus the mirror) of our simulated gamma-ray light curves that result from the sum of all mirroring events and include the contribution of the standard IC from the BLR. Note that such light curves feature several very bright and short spikes rising on timescales of a few minutes, as fit to explain the A16 observations of 3C 279.

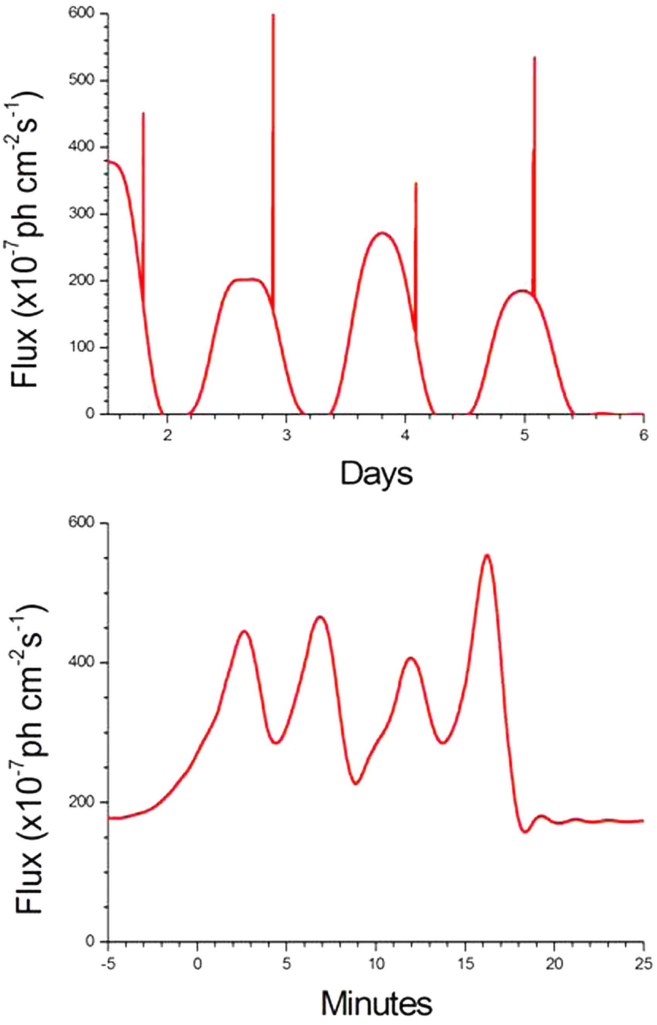

Figure 2. Gamma-ray light curves from our simulations based on the moving mirror model for the gamma-ray source in 3C 279. Upper panel: the simulated light curve over a several-day timescale to be compared with Figure 1 of A16. The emission spikes are the result of minute-timescale variability that is smoothed out for integration time bins of a few hours as used by A16. Lower panel: simulated light curve calculated for short timescales of the order of minutes, to be compared with Figure 2 of A16.

6. Discussion and Conclusions

The super-bright, super-fast, hard spectrum gamma-ray flares from 3C 279 in 2015 June call for a strong, compact source beyond the BLR. These requirements challenge radiative processes and source structures proposed over the years in the context of blazar emissions. Features of our model that meet the challenge include:

1. *Power and Compton dominance*. Very intense and fast gamma-ray flares are produced by the IC process beyond the BLR, arising from strongly enhanced density of reflected seed photons that are localized in mirror-plasmoid gaps along the jet. In fact, based on the photon energy density U'_m of Equation (8), we derive the energetics of the Compton-dominant flare and its requirements. To account for the intrinsic gamma-ray power $L_\gamma \sim 2 \times 10^{46}\,{\rm erg\,s^{-1}}$, we need an IC luminosity $L'_{IC} \simeq 5 \times 10^{43}\,{\rm erg\,s^{-1}}$ in the comoving frame. Since $L'_{IC} \simeq n'\,(4\pi/3)\ell'^3\,\sigma_T c\,U'\,\gamma^2_b$ holds, we require number densities of radiating electrons $n' \sim 10^2 \div 10^3\,{\rm cm^{-3}}$ with Lorentz factors up to $\gamma_b \sim 10^3$ and seed energy densities $U'_m \sim 10\,{\rm erg\,cm^{-3}}$ within the gaps that considerably exceed those prevailing in the BLR after Equation (2).
2. *Correlations*. The moving mirror mechanism naturally decouples the IC gamma-ray radiation produced in the gaps from the optical–UV emissions prevailing inside the BLR. This decoupling occurs on timescales $\simeq 2(R^*_m - \tilde{r})/c \sim$ half a day, so very large gamma-ray flares with Compton dominance $q \sim$ some 10^2 can be produced over and above a slowly varying background, as observed in 3C 279.

3. *Short timescales*. We follow the photon paths as shown in Figure 1: from S emission toward the mirror and backward from it. We obtain the risetime

$$t_v = (1+z)\, R_{\rm BLR}/(8c\,\Gamma^2\Gamma_r^2). \quad (9)$$

In our conditions given by $\Gamma \simeq 20$, $\Gamma_m \simeq 2$ and $R_{\rm BLR} \simeq 3\times 10^{17}$ cm, this comes to about 3 minutes, including the slowing down by the source redshift effect at $z = 0.536$.

4. *Hard, unabsorbed gamma-ray spectra*. We recall from the beginning of Section 4 that in the present context electron accelerations take place in the very same narrow gaps d_g (cf. Equation (3)) where the highest seed density is built up and the induced **E**-fields are largest. So the electrons can replenish their fast IC losses and retain a flat energy distribution. On the other hand, the IC upscattering of the mirrored photons occurs at radii beyond $R_{\rm BLR}$; there we evaluate the optical depth to photon–photon pair-producing interactions in the AGN frame from $\tau_{abs} \simeq \sigma_T\, U_m\, d_g/(3\,\epsilon) \sim 0.2$ (where $\epsilon \sim 1$ eV is the typical energy of the soft target photons) and obtain values smaller than unity even with conservative values $\Gamma \sim 20$.

We assume the plasmoids move along the jet following its opening angle $\theta \sim \Gamma^{-1}$, so the transversal size is $l' \simeq \theta R \simeq 10^{16}$ cm at the BLR edge and becomes a few times larger at the receiving point $\tilde{r} \sim 5\,10^{17}$ cm. The angular alignment between plasmoids and mirror $l'_m/\tilde{r} \sim 3\,10^{-2}$ implied by the model yields rare strong flickers over and above a much longer plateau, as indicated by the observations.

We note that the energetics required by the 2015 June event observed from 3C 279 that attained $E \simeq L'_\gamma\,\Gamma^2\,t_v \simeq$ a, few 10^{48} erg can be matched by a relativistic energy content of a plasmoid given by $E \simeq (4/3)\pi\,\ell'^3\,n'\,m_e\,c^2\,\gamma_b \sim$ a few 10^{48} erg, with $n' \sim 10^3$ cm^{-3}. This implies a pressure balancing that of the magnetic field and can be maintained by continued accelerations from magnetic reconnections, as computed and discussed by Petropoulou et al. (2016).

On the other hand, a mirror Compton reflectivity given by $f \simeq n'\sigma_T\, l'_m \sim$ a few % requires electron densities in the mirror around a few 10^6 cm^{-3}; this leads to a proton-dominated kinetic power $\pi\, l_m^2 c\, n' m_p c^2 \Gamma_m^2 \sim 10^{47}$ erg s^{-1} of the mirror. Note that deceleration and snow-plow effects through the jet will affect the leading mirror and help it to slow down toward small values $\Gamma_m \sim 2$ (see the end of Section 4). Such low values ensure a mirror contribution to the jet power below that of the other plasmoids, in spite of its higher density. So the total power carried by the jet is $L_j \sim 10^{47}$ erg s^{-1} close to the Eddington limit for a BH mass of $10^9\,M_\odot$. Such a value is at the upper end of the FSRQ range discussed by Celotti & Ghisellini (2008).

Virtues of our model include: boost values within $\Gamma \simeq 20$, as provided by the radio observations of 3C 279; standard values of the magnetic field $B \sim 1$ G; electron magnetization $\sigma_e > 10^2$, high enough as to allow efficient electron acceleration up to $\gamma \sim 10^3$ around or within plasmoids; and apparent gamma-ray luminosities up to 10^{49} erg s^{-1} from compact regions.

We acknowledge partial support through the ASI grant No. I/028/12/2.

References

Ackermann, M., Anantua, R., Asano, K., et al. 2016, ApJL, 824, L20 (A16)
Albert, J., Aliu, E., Anderhub, H., et al. 2008, Sci, 320, 1752
Aleksić, J., Antonelli, L. A., Antoraz, P., et al. 2011, ApJL, 730, L8
Böttcher, M., & Dermer, C. D. 1998, ApJL, 501, L51
Böttcher, M., Reimer, A., Sweeney, K., & Prakash, A. 2013, ApJ, 768, 54
Burch, J. L., Torbert, R. B., Phan, T. D., et al. 2016, Sci, 352, aaf2939
Cavaliere, A., Tavani, M., & Vittorini, V. 2017, ApJ, 836, 220
Celotti, A., & Ghisellini, G. 2008, MNRAS, 385, 283
Coppi, P. 2016, Talk Presented at the 14th AGILE Meeting, AGILE on the Wave, Rome, 2016 June 20–21, http://www.asdc.asi.it/14thagilemeeting/program.php
Costamante, L. 2017, Talk Presented at the 15th AGILE Meeting, Rome, 2017 May 23–24, http://www.asdc.asi.it/15thagilemeeting/program.php
Ghisellini, G., & Madau, P. 1996, MNRAS, 280, 67
Giuliani, A., D'Ammando, F., Vercellone, S., et al. 2009, A&A, 494, 509
Hartmann, R. C., Bertsch, D. L., Fichtel, C. E., et al. 1992, ApJL, 385, L1
Hayashida, M., Madejski, G. M., Nalewajko, K., et al. 2012, ApJ, 754, 114
Hayashida, M., Nalewajko, K., Madejski, G. M., et al. 2015, ApJ, 807, 79
Howatta, T., Valtaoja, E., Tornikoski, M., & Lähteenmäki, A. 2009, A&A, 494, 527
Kagan, D., Sironi, L., Cerutti, B., & Giannios, D. 2015, SSRv, 191, 545
Kniffen, D. A., Bertsch, D. L., Fichtel, C. E., et al. 1993, ApJ, 411, 133
Lyutikov, M., Sironi, L., Komissarov, S., & Porth, O. 2016, arXiv:1603.05731
MacDonald, N. R., Marscher, A. P., Jorstad, S. G., & Joshi, M. 2015, ApJ, 804, 111
Maraschi, L., Ghisellini, G., & Celotti, A. 1992, ApJL, 397, L5
Mignone, A., Striani, E., Tavani, M., & Ferrari, A. 2013, MNRAS, 436, 1102
Paliya, V. S. 2015, ApJL, 808, L48
Peterson, B. M. 1997, Active Galactic Nuclei, Vol. 117 (Cambridge: Cambridge Univ. Press), 314
Peterson, B. M. 2006, in The Broad-Line Region in Active Galactic Nuclei (Berlin: Springer), 77
Petropoulou, M., Giannios, D., & Sironi, L. 2016, MNRAS, 462, 3325
Rybicki, G. H., & Lightman, A. P. 1979, Radiative Processes in Astrophysics (New York: Wiley)
Sikora, M., Rutkowski, M., & Begelman, M. C. 2016, MNRAS, 457, 1352
Tavani, M., Vittorini, V., & Cavaliere, A. 2015, ApJ, 814, 51
Tavecchio, F., & Ghisellini, G. 2008, MNRAS, 385, L98
Vittorini, V., Tavani, M., Cavaliere, A., Striani, E., & Vercellone, S. 2014, ApJ, 793, 98
Yuan, Y., Nalewajko, K., Zrake, J., et al. 2016, ApJ, 828, 92